Title Page

miR-181c-BRK1 axis plays a key role in actin cytoskeleton-dependent T cell function

Shok Ping Lim,[*] Nikolaos Ioannou,[*] Alan G Ramsay,[*] David Darling,[*] Joop Gäken,[*, 1] and Ghulam J Mufti[*, †, 1]

[*]Department of Haemato-Oncology, Division of Cancer Studies, Faculty of Life Sciences & Medicine, King's College London, London, United Kingdom

[†]Department of Haemato-Oncology, King's College Hospital, London, United Kingdom

[1]Corresponding authors

Summary sentence: *miR-181c* modulates actin polymerization-mediated T cell functions through its regulation of BRK1

Running title: *miR-181c*-BRK1 axis in T cell actin dynamics

Correspondence: Ghulam J Mufti; Department of Haemato-Oncology, King's College London, Rayne Institute, 123 Coldharbour Lane, London SE5 9NU, United Kingdom; phone: +44(0)2032993080; fax: +44(0)2032993514; e-mail: ghulam.mufti@kcl.ac.uk and Joop Gäken; Department of Haemato-Oncology, King's College London, Rayne Institute, 123 Coldharbour Lane, London SE5 9NU, United Kingdom; phone: +44(0)2078485839; e-mail: joop.gaken@kcl.ac.uk

Keywords: T lymphocytes, microRNA, BRK1, F-actin

Total character count: 26496

Total number of figures: 6

Total number of color figures: 4

Total number of reference: 29

Total number of words in abstract: 222

Total number of words in summary sentence: 12

Abbreviations Page

BRK1: BRICK1, SCAR/WAVE Actin-Nucleating Complex Subunit

F-actin: filamentous actin

miRNA: microRNA

shRNA: short hairpin RNA

TCR: T cell receptor

WAVE: Wiskott-Aldrich Syndrome Protein (WASP) Family Verprolin-Homologous Protein

Abstract

MicroRNAs are short endogenous non-coding RNAs that play pivotal roles in a diverse range of cellular processes. The *miR-181* family is important in T cell development, proliferation and activation. In this study, we have identified BRK1 as a potential target of *miR-181c* using a dual selection functional assay and have showed that *miR-181c* regulates BRK1 by translational inhibition. Given the importance of *miR-181* in T cell function and the potential role of BRK1 in the involvement of WAVE2 complex and actin polymerization in T cells, we therefore investigated the influence of *miR-181c*-BRK1 axis in T cell function. Stimulation of PBMC derived $CD3^+$ T cells resulted in reduced *miR-181c* expression and upregulation of BRK1 protein expression, suggesting that *miR-181c*-BRK1 axis is important in T cell activation. We further showed that overexpression of *miR-181c* or suppression of *BRK1* resulted in inhibition of T cell activation and actin polymerization coupled with defective lamellipodia generation and immunological synapse formation. Additionally, we found that *BRK1* silencing led to reduced expressions of other proteins in the WAVE2 complex, suggesting that the impairment of T cell actin dynamics were a result of the instability of the WAVE2 complex following *BRK1* depletion. Collectively, we demonstrated that *miR-181c* reduces BRK1 protein expression level and highlighted the important role of *miR-181c*-BRK1 axis in T cell activation and actin polymerization-mediated T cell functions.

Introduction

MicroRNAs (miRNAs) are short endogenous non-coding RNAs which influence gene expression and play pivotal roles in a diverse range of cellular processes [1, 2]. We focused on the *miR-181* family which has previously been reported to play an important role in T cell functions [3-5]. The *miR-181* family consists of four members, *miR-181a*, *miR-181b*, *miR-181c* and *miR-181d*. *miR-181a* and *miR-181b* are localized on chromosome 1 (1q32.1) and chromosome 9 (9q33.3), while *miR-181c* and *miR-181d* are localized on chromosome 19 (19p13.12) [6]. *miR-181a* is an intrinsic modulator of the T cell receptor (TCR) signaling pathway by downregulating multiple negative regulators (phosphatases such as *PTPN22*, *SHP-2* and *DUSP6*) in the TCR signaling pathway. This dampens LCK and ERK signaling which in turn enhances the T cell activation [3]. Furthermore, *miR-181a/b*-deficient mice have a reduced number of T cells suggesting that *miR-181a* and *miR-181b* may be important in T cell development [4]. Overexpression of *miR-181c* in Jurkat and $CD4^+$ T cells was found to impair T cell activation and proliferation by reducing *IL-2* expression [5].

BRK1 (BRICK1, SCAR/WAVE Actin-Nucleating Complex Subunit) is a component of the WAVE [Wiskott-Aldrich Syndrome Protein (WASP) Family Verprolin-Homologous Protein] complex that plays a critical role in actin nucleation [7]. The WAVE regulatory complex at the N-terminal of WAVE protein consists of WAVE1/2/3, ABI1/2/3, SRA1, HEM1/2 and BRK1 [8, 9]. WAVE protein is a member of the WASP family, which recruits actin monomers (G-actin) and triggers conformational changes in ARP2/3 complex, thereby promoting production of branched networks of filamentous actin (F-actin) [7, 10].

The ability of T cells to polymerize actin is critical from the very first step of TCR engagement to the completion of a successful T cell activation [11]. Among the three isoforms of WAVE [12, 13], WAVE2 has been shown to be the major isoform expressed in T cells [14, 15] and increasing data has indicated that it is an essential regulator of multiple

actin cytoskeleton-dependent processes during T cell activation [14-17]. Suppression of *WAVE2* in Jurkat T cells has been shown to reduce the F-actin accumulation at the immunological synapse, decrease conjugate formation and cause defects in stable lamellipodia generation [14, 15]. In addition, loss of *WAVE2* in Jurkat T cells also led to reduction in IL-2 promoter activity and impairment in the regulation of Ca^{2+} [14]. Furthermore, silencing of *WAVE2* also caused defective integrin-mediated adhesion in primary $CD4^+$ T cells and Jurkat T cells in response to TCR activation [16, 17].

We identified the potential targets of *miR-181c/d* using an in-house functional assay [18]. This assay depends upon the functional activity rather than relying solely on the complementary binding of a miRNA to its putative target [19, 20]. In addition, this methodology is also able to identify targets that are downregulated by mRNA degradation or translational repression [18]. In this study, we focused on validating the downstream targets of *miR-181c* and investigating the biological functions of the identified targets. We demonstrated that the *miR-181c*-BRK1 axis plays an indispensable role in regulating T cell actin dynamics and thus is important in T cell activation, lamellipodia generation and immunological synapse formation.

Materials and Methods

Cell culture

Adherent cell lines (MCF7 and HeLa) were cultured in Dulbecco modified essential medium (DMEM) (Thermo Fisher Scientific, Waltham, MA, USA) whilst the suspension cell line (Jurkat T cells) was cultured in RPMI 1640 medium (Thermo Fisher Scientific). Both media were supplemented with 10% fetal bovine serum (FBS; Sigma-Aldrich, St. Louis, MO, USA) and 1% L-Glutamine-Penicillin-Streptomycin solution (Sigma-Aldrich). Isolation of primary $CD3^+$ T cells from peripheral blood mononuclear cells (PBMC) was performed using Dynabeads® Untouched™ Human T Cell Kit (Thermo Fisher Scientific). Isolated $CD3^+$ T cells were cultured in X-Vivo™15 medium (Lonza, Basel, Switzerland) supplemented with 2% human AB serum (Sigma-Aldrich) and 100U/ml recombinant human IL-2 (PeproTech, Rocky Hill, NJ, USA). Cells were cultured under humidified conditions at 37°C in 5% CO_2. Stimulation of Jurkat T cells was achieved with 10μg/ml of plate bound anti-human CD3 (clone OKT3; eBioscience, San Diego, CA, USA) and 25ng/ml of phorbol 12-myristate 13-acetate (PMA; Sigma-Aldrich) whilst primary T cells were stimulated with 2μg/ml of plate bound anti-human CD3 (clone OKT3; eBioscience) and 2μg/ml of soluble anti-human CD28 (clone 28.2; eBioscience).

Functional assay for *miR-181c/d* target identification

Functional assay to identify the target genes of *miR-181c/d* was performed as previously described [18]. The 3'UTR cDNA target ID library (MREH01; Sigma-Aldrich) derived from multiple human tissues and 10 human cell lines, representing 16,923 unique genes, was cloned downstream of a thymidine kinase-zeocin (TKzeo) fusion gene into in the p3'TKzeo vector, conferring zeocin resistance and ganciclovir (GCV) sensitivity. MCF7 cell line, expressing low levels of *miR-181c* and *miR-181d*, was transfected with this cDNA library

and selected with 100μg/ml zeocin (InvivoGen, San Diego, CA, USA), which results in a population of cells that express the TKzeo fusion gene from stably integrated library constructs. Expanded zeocin resistant cells were hence transfected with pBabePuro plasmid expressing *miR-181c/d*. After selection for stable integration with 2μg/ml puromycin (InvivoGen) and cell expansion, cells underwent subsequent GCV counter-selection. Genomic DNA was isolated from the expanded GCV resistant cells using Quick-gDNA™ MiniPrep Kit (Zymo Research, Irvine, CA, USA) and the cDNA containing *miR-181c/d* target sites was PCR amplified using p3'TKzeo specific primers flanking the cloning site (forward: 5'-GGGTCGACCTCGAATCCTTA-3'; reverse: 5'-CGAGGCGGCCGACATGTTT-3'). Amplified bands were purified, sequenced and aligned against human genome and transcript database in NCBI Nucleotide Blast to identify the putative targets of *miR-181c/d*. miRNA target identification and validation were performed as previously described [18].

Cell transfection and transduction

Ectopic expression of *miR-181* in MCF7, HeLa and Jurkat T cells was performed by transfecting the cells with 2μg of pBabePuro plasmid expressing *miR-181* using Ingenio® Electroporation Kit (Mirus Bio LLC, Madison, WI, USA). Cells transfected with empty pBabePuro vector were used as negative control. Transfected cells were then selected with 2μg/ml puromycin (InvivoGen). Transient transfection of cells with 100nM hsa-miR-181c-5p miRIDIAN hairpin inhibitor and negative control (Dharmacon, Lafayette, CO, USA) were also performed using the Ingenio® Electroporation Kit (Mirus Bio LLC). Suppression of *BRK1* in Jurkat and primary T cells was achieved by transducing the cells with short hairpin RNA (shRNA) lentiviral vectors (pLKO.1-shBRK1_1 and pLKO.1-shBRK1_2) in the presence of 4μg/ml of polybrene (Sigma-Aldrich). Cells transduced with pLKO.1-scrambled shRNA were used as negative control. For primary T cells, cells were stimulated with 2μg/ml

of plate bound anti-human CD3 (clone OKT3; eBioscience) and 2µg/ml of soluble anti-human CD28 (clone 28.2; eBioscience) before lentivirus transduction. shRNA lentivirus were generated by co-transfection of the human embryonic kidney HEK293T cell line with four plasmids; pMDG (envelope plasmid encoding VSV-G), pRRE (packaging plasmid encoding Gag & Pol), pREV (packaging plasmid encoding REV) and the shRNA plasmids (pLKO.1-shBRK1_1, pLKO.1-shBRK1_2 or pLKO.1-scrambled shRNA) using Calcium Phosphate Transfection Kit (Thermo Fisher Scientific).

Dual luciferase activity assay

Full length BRK1 was inserted downstream of a firefly luciferase gene (*luc2*) in the pmirGLO Dual-Luciferase miRNA Target Expression Vector (Promega, Madison, WI, USA). The pmirGLO-BRK1 construct was then transfected into *miR-181c* overexpressing MCF7, HeLa and Jurkat T cell lines. Transfection in MCF7 and HeLa cells were done using Ingenio® Electroporation Kit (Mirus Bio LLC) while transfection of Jurkat T cells was performed using Lipofectamine 2000 (Thermo Fisher Scientific). Firefly and *renilla* luciferase activities were measured 24 hours after transfection using the Dual-Glo® Luciferase Assay System (Promega). Normalized data were calculated as the ratio of firefly/*renilla* luciferase activities.

Flow cytometry analysis

Surface staining was performed with anti-human CD69-PE (eBioscience), Pacific Blue™ anti-human CD69 (BioLegend, San Diego, CA, USA) and anti-human CD154-PE (eBioscience) for an hour in the dark. F-actin was stained with rhodamine phalloidin (Thermo Fisher Scientific). Stained cells were washed and resuspended in FACS buffer (2.5% FBS in PBS) and analyzed on a BD FACSCanto II (BD Biosciences, San Jose, CA, USA). FlowJo Version 9.7.7 software (Tree Star, Ashland, OR, USA) was used to perform data analysis.

Spreading assay

8-well chamber culture slides (BD Falcon, San Jose, CA, USA) were coated with 0.01% poly-L-lysine solution (Sigma-Aldrich) for 15 minutes at room temperature and subsequently with 10μg/ml anti-human CD3 (clone OKT3; eBioscience) overnight at 4°C. 0.5×10^6 (for 1 minute of spreading) or 0.2×10^6 (for 3 and 5 minute of spreading) cells were plated gently onto the slides and allowed to spread for 1, 3 or 5 minutes. Cells were fixed with 4% paraformaldehyde for 30 minutes, permeabilized with 0.1% Triton X-100 in PBS for 5 minutes and blocked with 5% goat serum in 10% FBS/0.02% sodium azide in PBS for an hour. Cells were then stained with rhodamine phalloidin (Thermo Fisher Scientific) according to the manufacturer's instructions. After washing, the cell specimens were mounted with Vectashield Mounting Medium with DAPI (Vector Laboratories, Burlingame, CA, USA). Slides were analyzed using Leica DM4500B fluorescence microscope (Leica Microsystems, Wetzlar, Germany) with a 100× oil objective. Images were acquired using a Leica DFC365 FX monochrome digital camera and Leica LAS AF software. Percentage of spreading was calculated by counting at least 100 cells per experimental condition. Cells that form an F-actin ring at the cell periphery were scored as positive while cells without an F-actin ring were scored as negative.

Immunological synapse assay

MEC-1 B cells were stained with CellTracker Blue CMAC (Thermo Fisher Scientific) according to the manufacturer's instructions and pulsed with 2μg/mL of a cocktail of staphylococcal superantigens (sAgs; SEA and SEB; Sigma-Aldrich) for 30 minutes at 37°C. 1×10^6 of B cells were centrifuged at 200×g for 5 min with an equal number of T cells and incubated at 37°C for 15 minutes. Cells were transferred onto microscopic slides (Menzel-Glaser Polysine slides; Thermo Fisher Scientific) using a cell concentrator and fixed with 3% methanol-free formaldehyde (TABB Laboratories, Berks, England) in PBS for 15 minutes.

Subsequently, cells were permeabilized with 0.3% Triton X-100 in PBS for 5 minutes and treated with blocking buffer (0.1% BSA in PBS) for 10 minutes. F-actin was stained with rhodamine phalloidin (Thermo Fisher Scientific) according to the manufacturer's instructions. After washing, the cell specimens were sealed with 22mm×32mm coverslips using fluorescent mounting medium (Dako, Glostrup Municipality, Denmark). Medial optical section images were captured using an A1R confocal microscope (Nikon, Minato, Tokyo, Japan) with a 60×/1.40 oil objective by NIS-elements imaging software (Nikon). Detectors were set to detect an optimal signal below saturation limits. Fluorescence was acquired sequentially to prevent passage of fluorescence from other channels (Multi-Track). Image sets to be compared were acquired during the same session using identical acquisition settings. Blinded confocal images were analyzed using NIS-elements imaging software (Nikon). T cell-B cell conjugates were identified only when T cells were in direct contact interaction with B cells (blue fluorescent channel) and the total area (in square micrometers) of F-actin (red fluorescent channel) accumulation at all T cell contact sites and synapses with B cell was measured.

Quantitative real time PCR

Total RNA was extracted from cells using TRIzol (Thermo Fisher Scientific) method or RNeasy® Micro Kit (Qiagen, Germantown, MD, USA). For quantification of *BRK1* mRNA expression, first strand cDNA was synthesized using SuperScript® VILO™ cDNA Synthesis Kit (Thermo Fisher Scientific) and quantitative real time PCR (qPCR) analysis was carried out using the FastStart Universal Probe Master (ROX) and Universal Library Probes (Roche Diagnostics, Atlanta, GA, USA). The details of primers and probes used are shown in Supplemental Table 1. *BRK1* expression levels, normalized to *GAPDH*, were quantified with the relative quantification method ($2^{-\Delta\Delta Ct}$). For miRNA expression quantification, reverse transcription of miRNA was first carried out using Universal cDNA Synthesis Kit II (Exiqon,

Vedbæk, Denmark) and qPCR analysis was then performed using ExiLENT SYBR® Green Master Mix (Exiqon). Details of miRNA specific primer mix are shown in Supplemental Table 1. The *miR-181* levels were normalized to *miR-103a* and expressed as relative quantification ($2^{-\Delta\Delta Ct}$).

Western blot analysis

Whole cell lysates were prepared using 1× Radio-Immunoprecipitation Assay (RIPA) Lysis Buffer (Santa Cruz Biotechnology, CA, USA). 15-20µg of lysates were separated on NuPAGE™ Novex™ 4-12% Bis-Tris Protein Gels (Thermo Fisher Scientific), transferred to a PVDF membrane (Bio-Rad Laboratories, Hercules, CA, USA) and blocked with 5% non-fat dried milk in 0.1% Tween 20/PBS buffer for an hour. Membranes were then probed with mouse monoclonal anti-β-ACTIN (ab8226; Abcam, Cambridge, UK), mouse monoclonal anti-BRK1 (generous gift from Professor Stradal Theresia), rabbit polyclonal anti-WAVE2 (H-110; Santa Cruz Biotechnology), mouse monoclonal anti-ABI1 (C-1; Santa Cruz Biotechnology), rabbit polyclonal anti-PIR121-1/Sra-1 (EMD Millipore, Billerica, MA, USA), goat polyclonal anti-HEM1 (Q-12; Santa Cruz Biotechnology), rabbit polyclonal anti-ARP2 (H-84; Santa Cruz Biotechnology) and rabbit polyclonal anti-ARP3 (EMD Millipore) overnight at 4°C. After washing, membranes were subsequently probed with HRP-linked anti-rabbit IgG (Cell Signaling Technology, Danvers, MA, USA), HRP-linked anti-mouse IgG (Promega) and HRP-linked rabbit anti-goat IgG (Dako) for an hour at room temperature. Membranes were then incubated in Pierce™ ECL Western Blotting Substrate (Thermo Fisher Scientific) for 5 minutes and proteins were exposed to CL-Xposure™ Clear Blue X-ray Film (Thermo Fisher Scientific) for the preferable time using Photon Imaging Systems SRX-101A. Protein expression levels were quantified by Image Studio™ Lite Version 5 software (LI-COR Biosciences, Lincoln, NE, USA) against loading control (β-ACTIN) according to the band intensity.

Statistical analysis

Statistical analysis was performed using Prism Version 5 software (GraphPad Software Inc, La Jolla, CA, USA). Statistical significance was calculated by *P* value using unpaired t-test. *P* values <0.05 were considered statistically significant. Error bars were generated based on two to four independent experiments.

Online supplemental material

The online supplemental material consists of one supplemental table and four supplemental figures.

Results

miR-181c regulates BRK1 protein expression

To identify putative targets of *miR-181c/d*, we employed a functional screening assay which has been developed in-house [18]. cDNAs potentially targeted by *miR-181c/d* were PCR amplified from genomic DNA isolated from GCV resistant cells (Supplemental Figure 1A). Amplified bands were purified, sequenced and aligned against human genome and transcript database. A major transcript identified was *BRK1* (Supplemental Figure 1B).

Since *miR-181a*, *miR-181b*, *miR-181c* and *miR-181d* have the same seed sequence and they might regulate the same genes, we overexpressed *miR-181a*, *miR-181b*, *miR-181c* and *miR-181d* in three independent cells lines, MCF7, HeLa and Jurkat T cells (Figure 1A) in order to determine the mRNA and protein expressions of BRK1. We found that ectopic expressions of *miR-181a*, *miR-181b*, *miR-181c* and *miR-181d* had no impact on *BRK1* at the mRNA level in all three cell lines (Figure 1B). Nevertheless, BRK1 protein levels in MCF7, HeLa and Jurkat T cells were all substantially downregulated upon *miR-181c* overexpression (Figure 1C-D). However, in *miR-181a*, *miR-181b* and *miR-181d* overexpressing cells, the protein level of BRK1 was not altered (Figure 1C-D). These results indicate that only *miR-181c* regulates BRK1 protein expression. To further confirm that *miR-181c* regulates BRK1, *miR-181c* overexpressing MCF7, HeLa and Jurkat T cells underwent *miR-181c* inhibition by transfecting with miRIDIAN hairpin inhibitor directed against *miR-181c*. Analogous to *miR-181c* overexpression, *BRK1* expression remained unchanged at the mRNA level following *miR-181c* inhibition (Figure 1E). However, reduced BRK1 protein expression in *miR-181c* overexpressing cells could be reversed with *miR-181c* inhibition, resulting in a marked increase in protein expression of BRK1 (Figure 1F-G). Overall, these data demonstrated that overexpression and inhibition of *miR-181c* had no effect on the mRNA expression level of *BRK1* but did in fact modulate its protein expression, suggesting that *miR-181c* regulates

BRK1 expression by promoting translational inhibition rather than mRNA degradation. In addition, a dual luciferase reporter assay was also performed to further confirm that *miR-181c* regulates BRK1 expression. Luciferase activity from a plasmid with BRK1 cDNA cloned downstream of luciferase reduced significantly as a result of enforced expression of *miR-181c* in MCF7, HeLa and Jurkat T cells (Figure 1H), indicating that *miR-181c* represses BRK1 expression.

BRK1 is important for the stability of WAVE2 regulatory complex in T lymphocytes

In solid tumor cell lines, BRK1 has been shown to play an important role in regulating the stability of WAVE regulatory complex [21-23]. To explore whether BRK1 also plays a similar role in T lymphocytes, we examined the expressions of other proteins involved in WAVE2 complex including WAVE2, ABI1, SRA1 and HEM1 following knockdown of *BRK1* in both Jurkat and primary T cells. Upon suppression of *BRK1*, the protein levels of WAVE2, ABI1 and SRA1 were significantly reduced (Figure 2). However, HEM1 protein expression was not altered by *BRK1* depletion in both Jurkat and primary T cells (Figure 2). In addition, we also assessed whether BRK1 depletion would influence the levels of the components of ARP2/3 complex. We found that the protein expressions of ARP2 and ARP3 remained unchanged following BRK1 suppression (Figure 2). We also showed that reduced expression of BRK1 as a result of *miR-181c* overexpression in Jurkat T cells decreased the WAVE2 protein expression (Supplemental Figure 2). This data suggests that, as in solid tumor cell lines, BRK1 is important for the stability of other proteins in the WAVE2 regulatory complex in T cells.

***miR-181c*-BRK1 axis is important for T cell activation**

It has been shown that *miR-181*c is important in T cell activation [3, 5]. In this study, we found that *miR-181c* regulates the expression of BRK1. BRK1 is a component of the

WAVE2 complex which has been shown to be involved in T cell activation by modulating processes such as lamellipodia formation, immunological synapse formation, IL-2 promoter activity, integrin activation and Ca^{2+} entry [14-17]. Therefore, to study whether the regulation of BRK1 by *miR-181c* correlates with T cell activation, we examined the expression of *miR-181c* and BRK1 in PBMC derived $CD3^{+}$ T cells before and after co-stimulation with CD3 and CD28 antibodies. Following co-stimulation, the expression of *miR-181c* was reduced (Figure 3A) and BRK1 protein expression was upregulated (Figure 3B-C), suggesting that the *miR-181c*-BRK1 axis is important in T cell activation. To further examine the role of *miR-181c*-BRK1 axis in T cell activation, we overexpressed *miR-181c* (Supplemental Figure 3) and suppressed *BRK1* (Figure 3D) in Jurkat T cells. Subsequently, we analyzed the expression of CD69, a marker for T cell activation. Upon stimulation, the CD69 expression in Jurkat T cells was elevated as compared to its expression before stimulation. However, in the *miR-181c* overexpressing Jurkat T cells, the upregulation of CD69 expression was lower in comparison to control (Figure 3E). To quantitatively determine the effect of *miR-181c* overexpression on T cell activation, the mean fluorescence intensity (MFI) was analyzed indicative of CD69 expression. Following stimulation, the relative MFI of CD69 staining was increased both in control and *miR-181c* overexpressing cells in comparison to before stimulation. Nevertheless, the *miR-181c* overexpressing cells have a significantly lower increment of CD69 MFI as compared to control (Figure 3F). Similarly, the increment of CD69 expression in *BRK1*-suppressed Jurkat T cells (shBRK1_1 and shBRK1_2) was lower as compared to scrambled (Figure 3G-H). In addition, knockdown of *BRK1* was also performed in primary T cells (Supplemental Figure 4) where expression of CD69 (Figure 3I-J) and CD154 (Figure 3K-L) was also impaired following stimulation. Together, these data indicate that enforced expression of *miR-181c* or silencing of *BRK1* reduces CD96 and CD154 expression suggesting that *miR-181c*-BRK1 axis is involved in T cell activation.

miR-181c-BRK1 axis is required for actin polymerization in T cells

Reorganization of the actin cytoskeleton is a requisite event in controlling T cell activation and is critical for multiple aspects in T cell function [11]. Our finding on the involvement of *miR-181c*-BRK1 axis in T cell activation has led us to investigate whether F-actin polymerization during T cell activation is altered following ectopic expression of *miR-181c* and silencing of *BRK1*. We analyzed the total cellular F-actin content in *miR-181c* overexpressing and *BRK1*-silenced Jurkat and primary T cells before and after stimulation. Upon stimulation, the total cellular F-actin content in both control-transfected and *miR-181c* overexpressing Jurkat T cells was increased. However, a lower increment of the total cellular F-actin content was observed in *miR-181c* overexpressing cells in comparison to control (Figure 4A). To quantitatively determine the effect of *miR-181c* overexpression on actin polymerization, the MFI was analyzed indicative of the total cellular F-actin content. The relative MFI of F-actin staining was elevated in both control-transfected and *miR-181c* overexpressing Jurkat T cells following stimulation. Nonetheless, the *miR-181c* overexpressing cells have a significantly lower increment of F-actin MFI in comparison to control (Figure 4B). Similar to *miR-181c* overexpression, the increment of total cellular F-actin content in the *BRK1*-silenced cells was also significantly lower as quantified by MFI in both Jurkat (Figure 4C-D) and primary T cells (Figure 4E-F). Collectively, these data suggest that the *miR-181c*-BRK1 axis is required for maximal actin polymerization in T cells.

miR-181c-BRK1 axis plays a key role in lamellipodia formation in T lymphocytes

The effects of *miR-181c* or BRK1 modulation on the total cellular F-actin content in T cell activation have led us to determine whether enforced expression of *miR-181c* or knockdown of *BRK1* could have an impact on actin polymerization-mediated T cell functions. Spreading of T cells on anti-TCR coated slide requires the formation of stable actin structures and the generation of lamellipodia [24]. We thus assessed the ability of T cells to generate

lamellipodia using a spreading assay following *miR-181c* overexpression or *BRK1* suppression. We found that, during the spreading process, *miR-181c* overexpressing cells failed to spread on anti-CD3 coated slides whilst control cells were able to spread in a highly ordered fashion, forming a round lamellipodial interface at the cell periphery containing radially-arrayed F-actin-rich structures (Figure 5A). At the 1 minute time point, the percentage of cells that have spread on anti-CD3 coated slides in both control and *miR-181c* overexpression were all very low. Nevertheless, at 3 and 5 minutes, a significantly lower percentage of spreading was observed in *miR-181c* overexpressing cells as compared to control (Figure 5B). Consistent with this finding in *miR-181c* overexpression, in both Jurkat (Figure 5C-D) and primary T cells (Figure 5E-F), a small difference in percentage of spreading was seen at 1 minute between control and *BRK1*-knockdown T cells while significant differences were observed after 3 and 5 minutes of spreading where depletion of *BRK1* had a significant impact on the cell ability to spread in response to anti-CD3 stimulation. Taken together, these data suggest that the *miR-181c*-BRK1 axis is required for the generation of lamellipodia in response to TCR stimulation, a phenomenon requiring proper regulated actin polymerization.

miR-181c-BRK1 axis plays an important role in immunological synapse formation in T cells

The mutual recognition of the T cell and antigen presenting cell (APC) results in the engagement and clustering of the TCR, and the formation of the T cell-APC interface, known as the immunological synapse. Regulation of actin polymerization at the immunological synapse is crucial to initiate and sustain T cell activation. We therefore analyzed whether ectopic expression of *miR-181c* or suppression of *BRK1* could impair actin polymerization at the immunological synapse (T cell-B cell conjugation site). Our results showed that overexpression of *miR-181c* in Jurkat T cells led to severe impairment in actin

polymerization in response to stimulation with superantigen-pulsed MEC-1 B cells. In comparison to control, *miR-181c* overexpression resulted in a marked reduction of F-actin staining at the T cell-B cell contact site (Figure 6A). To quantitatively determine the effect of *miR-181c* overexpression on immunological synapse formation, we measured the total area (in square micrometers) of F-actin accumulation at T cell contact sites and synapses with B cells where a significant reduction in the total area of F-actin accumulation at T cell-B cell contact site was found (Figure 6B). Consistently, we also demonstrated that in both Jurkat (Figure 6C-D) and primary T cells (Figure 6E-F), knockdown of *BRK1* impaired the actin polymerization at the T cell-B cell contact site as shown by significantly reduced F-actin staining and total area of F-actin accumulation at the T cell-B cell synapses. Overall, these data suggest that the ectopic expression of *miR-181c* or silencing of *BRK1* impairs immunological synapse formation, a process that is highly dependent on proper regulation of actin cytoskeletal dynamics at the T cell-B cell conjugation site.

Discussion

In this study we show, for the first time, that *miR-181c* modulates BRK1 by translational inhibition. BRK1 is a component of the WAVE complex that regulates actin polymerization [7]. It has been confirmed that at the N-terminal of the WAVE protein, a tight pentameric complex consisting of WAVE1/2/3, ABI1/2/3, SRA1, HEM1/2 and BRK1 is formed [8, 9]. In this study, we showed that upon *BRK1* silencing, the protein expression levels of WAVE2, ABI1 and SRA1 were reduced in both Jurkat and primary T cells consistent with previous studies [21-23]. Derivery and colleagues demonstrated that siRNA knockdown of *BRK1* in HeLa cells resulted in a reduction of the protein expressions of WAVE2, SRA1, NAP1 and ABI1 [21] while in lung cancer PG cell line, Cai *et al.* reported that loss of *BRK1* resulted in decreased expression of WAVE2 protein [22]. Suppression of *BRK1* in osteosarcoma U2OS cell line also contributed to decreased protein expressions of ABI1, WAVE1 and WAVE2 [23]. Interestingly, we found that the HEM1 protein level was not altered following *BRK1* depletion. This might be due to the fact that BRK1 does not interact directly with HEM1 in the WAVE2 complex [8, 21, 25]. Previous studies have shown that BRK1 is a precursor in the assembly of WAVE-ABI-BRK1 heterotrimeric complex and in the subsequent binding of the heterotrimer to the SRA1-HEM1 dimer in order to form a functional WAVE regulatory complex. The binding of the WAVE-ABI-BRK1 heterotrimer to the SRA1-HEM1 dimer is mainly via interaction between BRK1 and SRA1 [8, 21, 25]. Thus, during the assembly of a WAVE regulatory complex, BRK1 interacts directly with WAVE, ABI and SRA1 proteins but not HEM1 protein. Furthermore, we also found that the ARP2 and ARP3 proteins levels remained unchanged following suppression of *BRK1* consistent with the fact that the ARP2/3 complex only binds to activated WAVE2 protein at its C-terminal end [7, 10]. Collectively, our data suggest that in T cells, *miR-181c* represses BRK1 expression which in turn destabilize proteins in the WAVE2 complex.

Upon stimulation of PBMC derived $CD3^+$ T cells, we found that the expression of *miR-181c* was significantly reduced and the protein expression of BRK1 was markedly elevated. Further overexpression and knockdown studies confirmed that the *miR-181c*-BRK1 axis is important in T cell activation. In addition, we demonstrated that the *miR-181c*-BRK1 axis regulates actin polymerization-dependent processes in T cells such as lamellipodia generation and immunological synapse formation.

Although the role of *miR-181c* in regulation of actin dynamics in T cells is poorly understood, there are several previous studies which showed that the *miR-181* family is important in T cell activation. *miR-181a* has been shown to enhance T cell activation by downregulating multiple negative regulators (phosphatases such as *PTPN22, SHP-2* and *DUSP6*) in the TCR signaling pathway [3]. In addition, downregulation of *miR-181c* expression following T cell activation has been previously reported in Jurkat and PBMC derived $CD4^+$ T cells [5]. Moreover, ectopic expression of *miR-181c* in Jurkat and $CD4^+$ T cells has been shown to reduce T cell activation and proliferation by targeting *IL-2* [5].

It is evident that BRK1 plays a key role in cellular processes that are dependent on actin cytoskeleton [26]. For example, BRK1 was shown to be required for lamellipodia formation in HeLa cells [21, 27]. Suppression of *BRK1* in non-small cell lung carcinoma cell line caused actin filament reorganization, inhibited pseudopodia formation and blocked cell migration [22]. Loss of *BRK1* in renal cell carcinoma and osteosarcoma cell lines also resulted in defective directional migration and invasive growth, coupled with reduced cell proliferation [23]. Furthermore, BRK1 is also essential in actin dynamics and cell survival during embryo development as genetic ablation of *Brk1* in mice resulted in dramatic defects in embryo compaction and development [23]. In addition, BRK1 regulates actin dynamics during the processes of neurite outgrowth in human neuroblastoma [28].

Although much remains unknown regarding the role of BRK1 in actin reorganization in T cells, the WAVE2 complex has been shown to be important in regulating actin cytoskeletal remodeling in T cells. Nolz and colleagues showed that *WAVE2* suppression resulted in reduction in conjugation formation and F-actin accumulation at the T cell-B cell site, coupled with defects in generation of stable lamellipodia in response to anti-TCR ligation [14]. In addition, the two members of WAVE2 complex, ABI2 and HEM1, have also been shown to be recruited at the immunological synapse site together with WAVE2 and F-actin, and loss of *HEM1* exhibited significant defects in conjugate formation similar to *WAVE2* suppression [14]. Moreover, Zipfel *et al.* demonstrated that ABI co-localizes with WAVE1 and WAVE2 at the sites of dynamic actin polymerization, including the leading edge of spreading T cells and the T cell-B cell conjugation site [15]. Similarly, primary T cell derived from *Abi1/Abi2*-deficient mice were also shown to exhibit reduced actin polymerization upon T cell activation [15] and *Hem1* deficiency in mice has been shown to result in impaired T cell activation, adhesion and development as well as defective F-actin polymerization and actin cap formation in lymphocytes [29].

In conclusion, we have showed that *miR-181c* regulates BRK1 protein expression level, however the exact direct or indirect mechanism needs to be further explored. In addition, we have also demonstrated the important role of *miR-181c*-BRK1 axis in actin polymerization-mediated T cell functions and T cell activation.

Authorship

SPL designed the study, performed the experiments, analyzed the results and prepared the manuscript; NI and AGR contributed to the immunological synapse assay; DD contributed to the lentivirus production; and JG and GJM designed the study, supervised the project and prepared the manuscript.

Acknowledgements

The authors would like to thank Dr Heba A Alkhatabi and Dr Austin G Kulasekararaj for contribution to the *miR-181c* target identification, Dr Stephen Orr and Dr Nermina Lamadema for help with the PBMC and $CD3^+$ T cell isolation, Dr Terry Gaymes for the Jurkat T cell line and Professor Stradal Theresia (Helmholtz Centre for Infection Research) for the BRK1 antibody.

Conflict of Interest Disclosure

The authors declare no conflict of interest.

References

1. Ambros, V. (2001) microRNAs: tiny regulators with great potential. Cell 107, 823-826.

2. Bartel, D. P. (2004) MicroRNAs: Genomics, Biogenesis, Mechanism, and Function. Cell 116, 281-297.

3. Li, Q.-J., Chau, J., Ebert, P. J., Sylvester, G., Min, H., Liu, G., Braich, R., Manoharan, M., Soutschek, J., Skare, P. (2007) miR-181a is an intrinsic modulator of T cell sensitivity and selection. Cell 129, 147-161.

4. Henao-Mejia, J., Williams, A., Goff, Loyal A., Staron, M., Licona-Limón, P., Kaech, Susan M., Nakayama, M., Rinn, John L., Flavell, Richard A. (2013) The MicroRNA miR-181 Is a Critical Cellular Metabolic Rheostat Essential for NKT Cell Ontogenesis and Lymphocyte Development and Homeostasis. Immunity 38, 984-997.

5. Xue, Q., Guo, Z.-Y., Li, W., Wen, W.-H., Meng, Y.-L., Jia, L.-T., Wang, J., Yao, L.-B., Jin, B.-Q., Wang, T., Yang, A.-G. (2011) Human activated CD4+ T lymphocytes increase IL-2 expression by downregulating microRNA-181c. Molecular Immunology 48, 592-599.

6. Ji, J., Yamashita, T., Budhu, A., Forgues, M., Jia, H. L., Li, C., Deng, C., Wauthier, E., Reid, L. M., Ye, Q. H. (2009) Identification of microRNA-181 by genome-wide screening as a critical player in EpCAM-positive hepatic cancer stem cells. Hepatology 50, 472-480.

7. Takenawa, T. and Suetsugu, S. (2007) The WASP-WAVE protein network: connecting the membrane to the cytoskeleton. Nature Reviews Molecular Cell Biology 8, 37-48.

8. Chen, Z., Borek, D., Padrick, S. B., Gomez, T. S., Metlagel, Z., Ismail, A. M., Umetani, J., Billadeau, D. D., Otwinowski, Z., Rosen, M. K. (2010) Structure and control of the actin regulatory WAVE complex. Nature 468, 533-538.

9. Gautreau, A., Ho, H.-y. H., Li, J., Steen, H., Gygi, S. P., Kirschner, M. W. (2004) Purification and architecture of the ubiquitous Wave complex. Proceedings of the National Academy of Sciences of the United States of America 101, 4379-4383.

10. Goley, E. D. and Welch, M. D. (2006) The ARP2/3 complex: an actin nucleator comes of age. Nature Reviews Molecular Cell Biology 7, 713-726.

11. Holsinger, L. J., Graef, I. A., Swat, W., Chi, T., Bautista, D. M., Davidson, L., Lewis, R. S., Alt, F. W., Crabtree, G. R. (1998) Defects in actin-cap formation in Vav-deficient mice implicate an actin requirement for lymphocyte signal transduction. Current Biology 8, 563-573.

12. Kurisu, S. and Takenawa, T. (2009) The WASP and WAVE family proteins. Genome Biology 10, 1.

13. Oda, A. and Eto, K. (2013) WASPs and WAVEs: From molecular function to physiology in hematopoietic cells. Seminars in Cell & Developmental Biology 24, 308-313.

14. Nolz, J. C., Gomez, T. S., Zhu, P., Li, S., Medeiros, R. B., Shimizu, Y., Burkhardt, J. K., Freedman, B. D., Billadeau, D. D. (2006) The WAVE2 Complex Regulates Actin Cytoskeletal Reorganization and CRAC-Mediated Calcium Entry during T Cell Activation. Current Biology 16, 24-34.

15. Zipfel, P. A., Bunnell, S. C., Witherow, D. S., Gu, J. J., Chislock, E. M., Ring, C., Pendergast, A. M. (2007) Role for the Abi/Wave Protein Complex in T Cell Receptor-Mediated Proliferation and Cytoskeletal Remodeling. Current Biology 16, 35-46.

16. Nolz, J. C., Medeiros, R. B., Mitchell, J. S., Zhu, P., Freedman, B. D., Shimizu, Y., Billadeau, D. D. (2007) WAVE2 Regulates High-Affinity Integrin Binding by Recruiting Vinculin and Talin to the Immunological Synapse. Molecular and Cellular Biology 27, 5986-6000.

17. Nolz, J. C., Nacusi, L. P., Segovis, C. M., Medeiros, R. B., Mitchell, J. S., Shimizu, Y., Billadeau, D. D. (2008) The WAVE2 complex regulates T cell receptor signaling to integrins via Abl- and CrkL-C3G-mediated activation of Rap1. The Journal of Cell Biology 182, 1231-1244.

18. Gäken, J., Mohamedali, A. M., Jiang, J., Malik, F., Stangl, D., Smith, A. E., Chronis, C., Kulasekararaj, A. G., Thomas, N. S. B., Farzaneh, F., Tavassoli, M., Mufti, G. J. (2012) A functional assay for microRNA target identification and validation. Nucleic Acids Research 40, e75.

19. Didiano, D. and Hobert, O. (2006) Perfect seed pairing is not a generally reliable predictor for miRNA-target interactions. Nature Structural & Molecular Biology 13, 849-851.

20. Bartel, D. P. (2009) MicroRNAs: target recognition and regulatory functions. Cell 136, 215-233.

21. Derivery, E., Fink, J., Martin, D., Houdusse, A., Piel, M., Stradal, T. E., Louvard, D., Gautreau, A. (2008) Free Brick1 is a trimeric precursor in the assembly of a functional wave complex. PLoS One 3, e2462.

22. Cai, X., Xiao, T., James, S. Y., Da, J., Lin, D., Liu, Y., Zheng, Y., Zou, S., Di, X., Guo, S., Han, N., Lu, Y.-J., Cheng, S., Gao, Y., Zhang, K. (2009) Metastatic potential of lung squamous cell carcinoma associated with HSPC300 through its interaction with WAVE2. Lung Cancer 65, 299-305.

23. Escobar, B., de Cárcer, G., Fernández-Miranda, G., Cascón, A., Bravo-Cordero, J. J., Montoya, M. C., Robledo, M., Cañamero, M., Malumbres, M. (2010) Brick1 Is an Essential Regulator of Actin Cytoskeleton Required for Embryonic Development and Cell Transformation. Cancer Research 70, 9349-9359.

24. Bunnell, S. C., Kapoor, V., Trible, R. P., Zhang, W., Samelson, L. E. (2001) Dynamic Actin Polymerization Drives T Cell Receptor-Induced Spreading: A Role for the Signal Transduction Adaptor LAT. Immunity 14, 315-329.

25. Linkner, J., Witte, G., Stradal, T., Curth, U., Faix, J. (2011) High-Resolution X-Ray Structure of the Trimeric Scar/WAVE-Complex Precursor Brk1. PLoS One 6, e21327.

26. Li, M., Ling, B., Xiao, T., Tan, J., An, N., Han, N., Guo, S., Cheng, S., Zhang, K. (2014) Sp1 transcriptionally regulates BRK1 expression in non-small cell lung cancer cells. Gene 542, 134-140.

27. Eden, S., Rohatgi, R., Podtelejnikov, A. V., Mann, M., Kirschner, M. W. (2002) Mechanism of regulation of WAVE1-induced actin nucleation by Rac1 and Nck. Nature 418, 790-793.

28. Wang, J.-L., Tong, C.-W., Chang, W.-T., Huang, A. M. (2013) Novel genes FAM134C, C3orf10 and ENOX1 are regulated by NRF-1 and differentially regulate neurite outgrowth in neuroblastoma cells and hippocampal neurons. Gene 529, 7-15.

29. Park, H., Staehling-Hampton, K., Appleby, M. W., Brunkow, M. E., Habib, T., Zhang, Y., Ramsdell, F., Liggitt, H. D., Freie, B., Tsang, M., Carlson, G., Friend, S., Frevert, C., Iritani, B. M. (2008) A point mutation in the murine Hem1 gene reveals an essential role for Hematopoietic Protein 1 in lymphopoiesis and innate immunity. The Journal of Experimental Medicine 205, 2899-2913.

Figure Legends

Figure 1. *miR-181c* regulates BRK1 expression. (A) qPCR analysis of relative *miR-181a*, *miR-181b*, *miR-181c* and *miR-181d* expressions in MCF7, HeLa and Jurkat T cells transfected with pBabePuro vector (control), pBabePuro plasmid expressing *miR-181a*, *miR-181b*, *miR-181c* and *miR-181d*. (B) qPCR analysis of relative *BRK1* mRNA expression in MCF7, HeLa and Jurkat T cells following *miR-181a*, *miR-181b*, *miR-181c* and *miR-181d* overexpression. (C) Western blot analysis of BRK1 protein expression in *miR-181a*, *miR-181b*, *miR-181c* and *miR-181d* overexpressing MCF7, HeLa and Jurkat T cells. β-ACTIN level is used as a loading control. (D) Densitometric quantification of BRK1 protein expression level normalized to β-ACTIN from three independent experiments. (E) qPCR analysis of relative *BRK1* mRNA expression in *miR-181c* overexpressing MCF7, HeLa and Jurkat T cells (control) and in *miR-181c* overexpressing MCF7, HeLa and Jurkat T cells following *miR-181c* inhibition. (F) Western blot analysis of BRK1 protein expression in *miR-181c* overexpressing MCF7, HeLa and Jurkat T cells following *miR-181c* inhibition. (G) Densitometric quantification of BRK1 protein expression level normalized to β-ACTIN from two independent experiments. (H) Relative firefly:*renilla* luciferase activity of BRK1 in *miR-181c* overexpressing MCF7, HeLa and Jurkat T cells. Error bars represent mean ± SD. * $P \leq .05$; ** $P \leq .01$; ns *P*=not significant.

Figure 2. BRK1 is important for stability of WAVE2 regulatory complex in T cells. (A) Western blots showing protein expressions of BRK1, WAVE2, ABI1, SRA1, HEM1, ARP2 and ARP3 in Jurkat and primary T cells transduced with scrambled shRNA (Scrambled) and two independent shRNA targeting *BRK1* (shBRK1_1 and shBRK1_2). β-ACTIN level is used as a loading control and numbers represent the densitometric quantification of protein expression levels normalized to β-ACTIN.

Figure 3. The *miR-181c*-BRK1 axis is involved in T cell activation. (A) qPCR analysis of relative *miR-181c* expression in PBMC derived $CD3^+$ T cells before and after stimulation with 2μg/ml of plate-bound anti-human CD3 and soluble anti-human CD28 antibodies for 24 hr. (B) Western blot analysis of BRK1 protein expression in PBMC derived $CD3^+$ T cells before and after stimulation. β-ACTIN level is used as a loading control. (C) Densitometric quantification of BRK1 protein expression level normalized to β-ACTIN from two independent experiments. (D) qPCR analysis of relative *BRK1* mRNA expression in Jurkat T cells transduced with scrambled shRNA (Scrambled) and two independent shRNA targeting *BRK1* (shBRK1_1 and shBRK1_2). (E) CD69 expression in Jurkat T cells transfected with pBabePuro vector (control) and pBabePuro plasmid expressing *miR-181c* before (red) and after (blue) stimulation with 10μg/ml plate-bound anti-human CD3 antibody and 25ng/ml PMA for 24 hr. (F) Chart showing the quantification of relative MFI of CD69 staining from three independent experiments. (G-H) CD69 expression in *BRK1*-knockdown Jurkat T cells before (red) and after (blue) stimulation. (I-J) CD69 and (K-L) CD154 expression in *BRK1*-suppressed primary T cells before (red) and after (blue) stimulation with 2μg/ml plate-bound anti-human CD3 and soluble anti-human CD28 antibodies for 24 hr. Y-axis indicates cell number and x-axis indicates log fluorescence intensity of CD69-PE, Pacific Blue CD69 or CD154-PE staining. Error bars represent mean ± SD. * $P \leq .05$; ** $P \leq .01$; *** $P \leq .001$.

Figure 4. Overexpression of *miR-181c* and silencing of *BRK1* reduced actin polymerization in T cells. (A) F-actin staining of *miR-181c* overexpressing Jurkat T cells before (red) and after (blue) stimulation with 10μg/ml plate-bound anti-human CD3 antibody and 25ng/ml PMA for 24 hr. Y-axis indicates cell number and x-axis indicates log fluorescence intensity of F-actin (rhodamine phalloidin) staining. (B) Chart showing the quantification of relative MFI of F-actin staining from three independent experiments. (C-D) Plots and charts showing the total F-actin cellular content in Jurkat T cells with *BRK1*

knockdown before (red) and after (blue) stimulation. (E-F) Plots and charts showing the total F-actin cellular content in *BRK1*-suppressed primary T cells before (red) and after (blue) stimulation with 2μg/ml plate-bound anti-human CD3 and soluble anti-human CD28 antibodies for 24 hr. Error bars represent mean ± SD. * $P \leq .05$.

Figure 5. Ectopic expression of *miR-181c* and suppression of *BRK1* caused defective lamellipodia formation in response to TCR stimulation during T cell spreading. (A) Microscopy images showing the lamellipodia formation in Jurkat T cells during cell spreading at 1, 3 and 5 min upon *miR-181c* overexpression. Cells were fixed, permeabilized, blocked and stained with rhodamine phalloidin (red) and DAPI (blue), followed by analysis using fluorescence microscopy with a 100× oil objective. (B) Chart showing the percentage of spreading at 1, 3 and 5 min. Statistical analysis is performed at 5 min time point. (C-D) Microscopy images and charts showing the spreading of Jurkat T cells upon *BRK1* silencing. Analysis is performed as in panels A-B. (E-F) Microscopy images and charts showing the spreading of primary T cells following *BRK1* knockdown. Analysis is performed as in panels A-B. Error bars represent mean ± SEM. ** $P \leq .01$; *** $P \leq .001$.

Figure 6. Enforced expression of *miR-181c* and depletion of *BRK1* impaired immunological synapse formation in T cells. (A) Confocal images showing the immunological synapse formation between *miR-181c* overexpressing Jurkat T cells (unstained) and superantigen-pulsed MEC-1 B cells (blue). Equal number of Jurkat T cells and superantigen-pulsed MEC-1 B cells were centrifuged, incubated, transferred to microscopic slides, fixed, permeabilized and blocked. F-actin was stained using rhodamine phalloidin (red) and slides were analyzed by confocal microscopy using a 60×/1.40 oil objective. (B) Chart showing the quantification of the total area of F-actin at the T cell-B cell contact site (white arrows) by NIS-elements imaging software. (C-D) Confocal images and charts showing the immunological synapse formation between *BRK1*-suppressed Jurkat T

cells and superantigen-pulsed MEC-1 B cells. Immunological synapse assay is performed and analyzed as in panels A-B. (E-F) Confocal images and charts showing the immunological synapse formation between *BRK1*-suppressed primary T cells and superantigen-pulsed MEC-1 B cells. Immunological synapse assay is performed and analysis is done as in panels A-B. Error bars represent mean $\pm$ SEM. * $P \leq .05$; ** $P \leq .01$; *** $P \leq .001$.

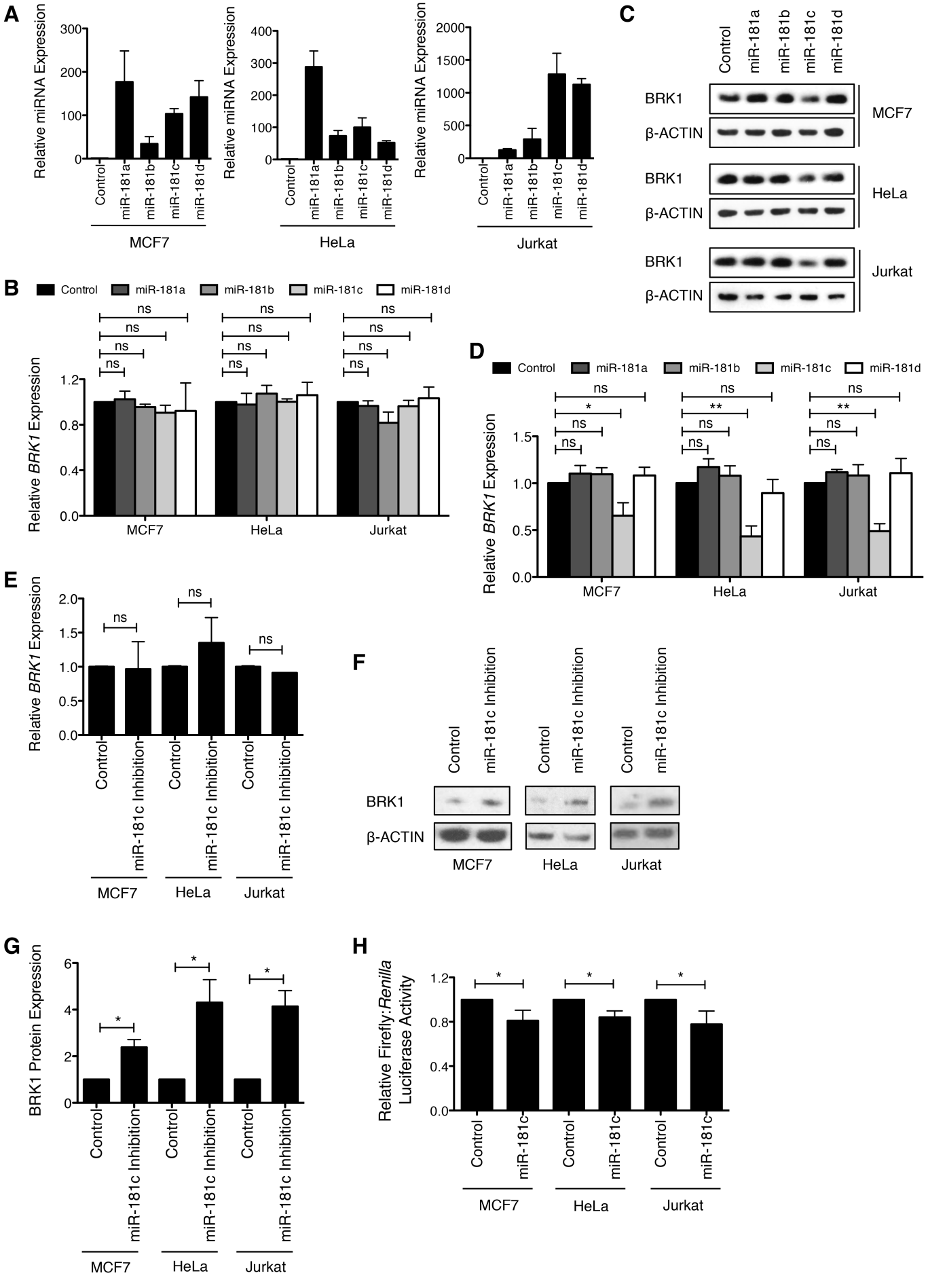
A
Relative miRNA Expression
Control
miR-181a
miR-181b
miR-181c
miR-181d
MCF7
HeLa
Jurkat
B
Relative BRK1 Expression
ns
C
BRK1
β-ACTIN
D
*
**
E
F
miR-181c Inhibition
G
BRK1 Protein Expression
H
Relative Firefly:Renilla Luciferase Activity

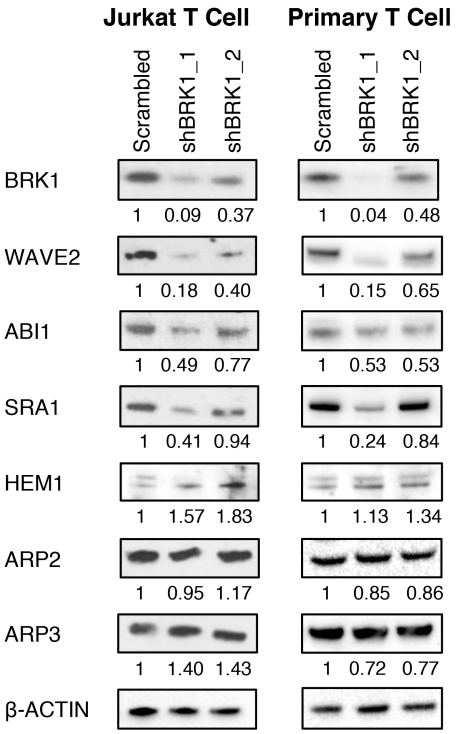
Jurkat T Cell
Primary T Cell
Scrambled
shBRK1_1
shBRK1_2
Scrambled
shBRK1_1
shBRK1_2
BRK1
1 0.09 0.37
1 0.04 0.48
WAVE2
1 0.18 0.40
1 0.15 0.65
ABI1
1 0.49 0.77
1 0.53 0.53
SRA1
1 0.41 0.94
1 0.24 0.84
HEM1
1 1.57 1.83
1 1.13 1.34
ARP2
1 0.95 1.17
1 0.85 0.86
ARP3
1 1.40 1.43
1 0.72 0.77
β-ACTIN

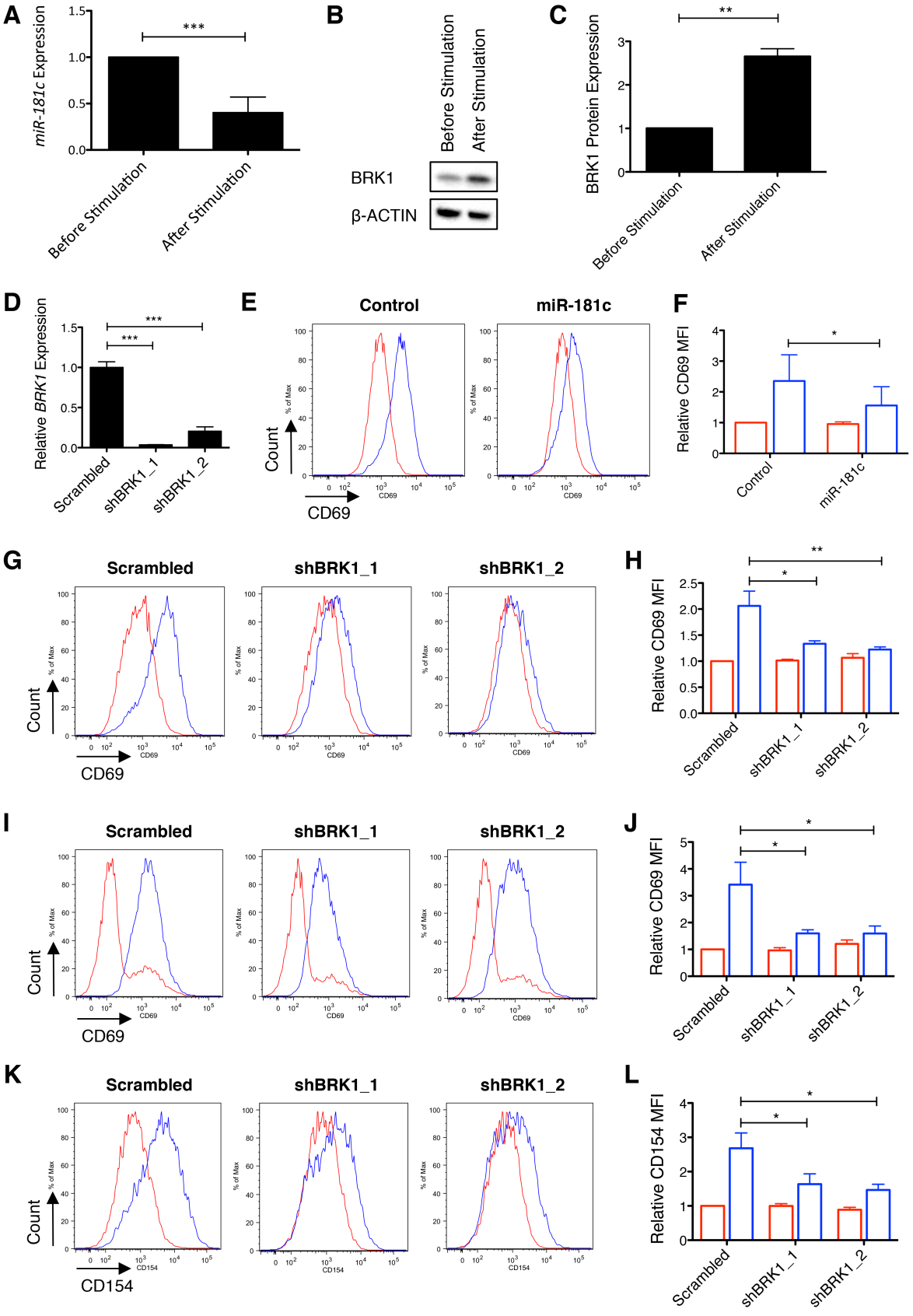
A
miR-181c Expression
1.5
1.0
0.5
0.0
***
Before Stimulation
After Stimulation
B
Before Stimulation
After Stimulation
BRK1
β-ACTIN
C
BRK1 Protein Expression
3
2
1
0
**
Before Stimulation
After Stimulation
D
Relative BRK1 Expression
1.5
1.0
0.5
0.0
***
***
Scrambled
shBRK1_1
shBRK1_2
E
Control
miR-181c
Count
% of Max
CD69
F
Relative CD69 MFI
4
3
2
1
0
*
Control
miR-181c
G
Scrambled
shBRK1_1
shBRK1_2
Count
% of Max
CD69
H
Relative CD69 MFI
2.5
2.0
1.5
1.0
0.5
0.0
**
*
Scrambled
shBRK1_1
shBRK1_2
I
Scrambled
shBRK1_1
shBRK1_2
Count
% of Max
CD69
J
Relative CD69 MFI
5
4
3
2
1
0
*
*
Scrambled
shBRK1_1
shBRK1_2
K
Scrambled
shBRK1_1
shBRK1_2
Count
% of Max
CD154
L
Relative CD154 MFI
4
3
2
1
0
*
*
Scrambled
shBRK1_1
shBRK1_2

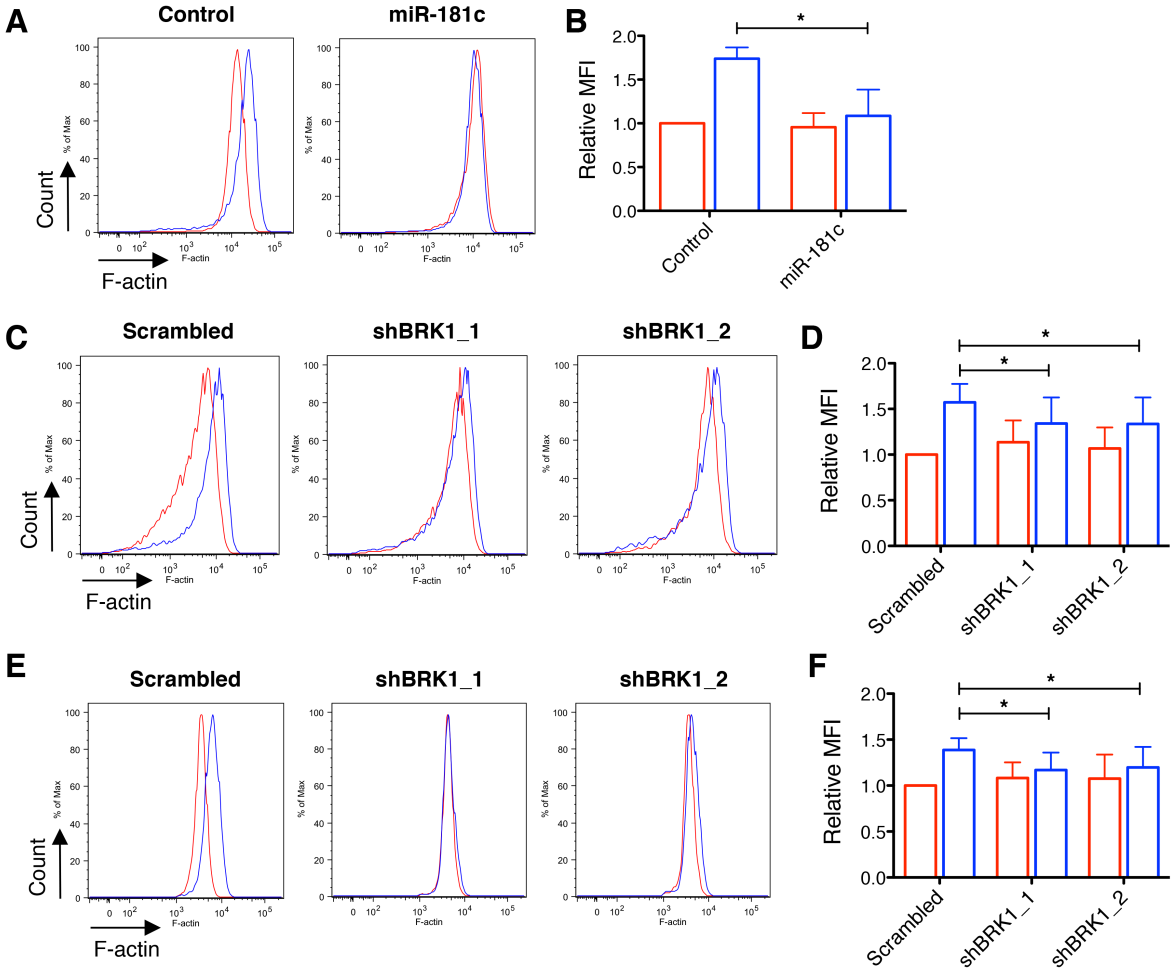
A
Control
miR-181c
Count
% of Max
F-actin
B
Relative MFI
Control
miR-181c
C
Scrambled
shBRK1_1
shBRK1_2
D
Relative MFI
Scrambled
shBRK1_1
shBRK1_2
E
Scrambled
shBRK1_1
shBRK1_2
F
Relative MFI
Scrambled
shBRK1_1
shBRK1_2

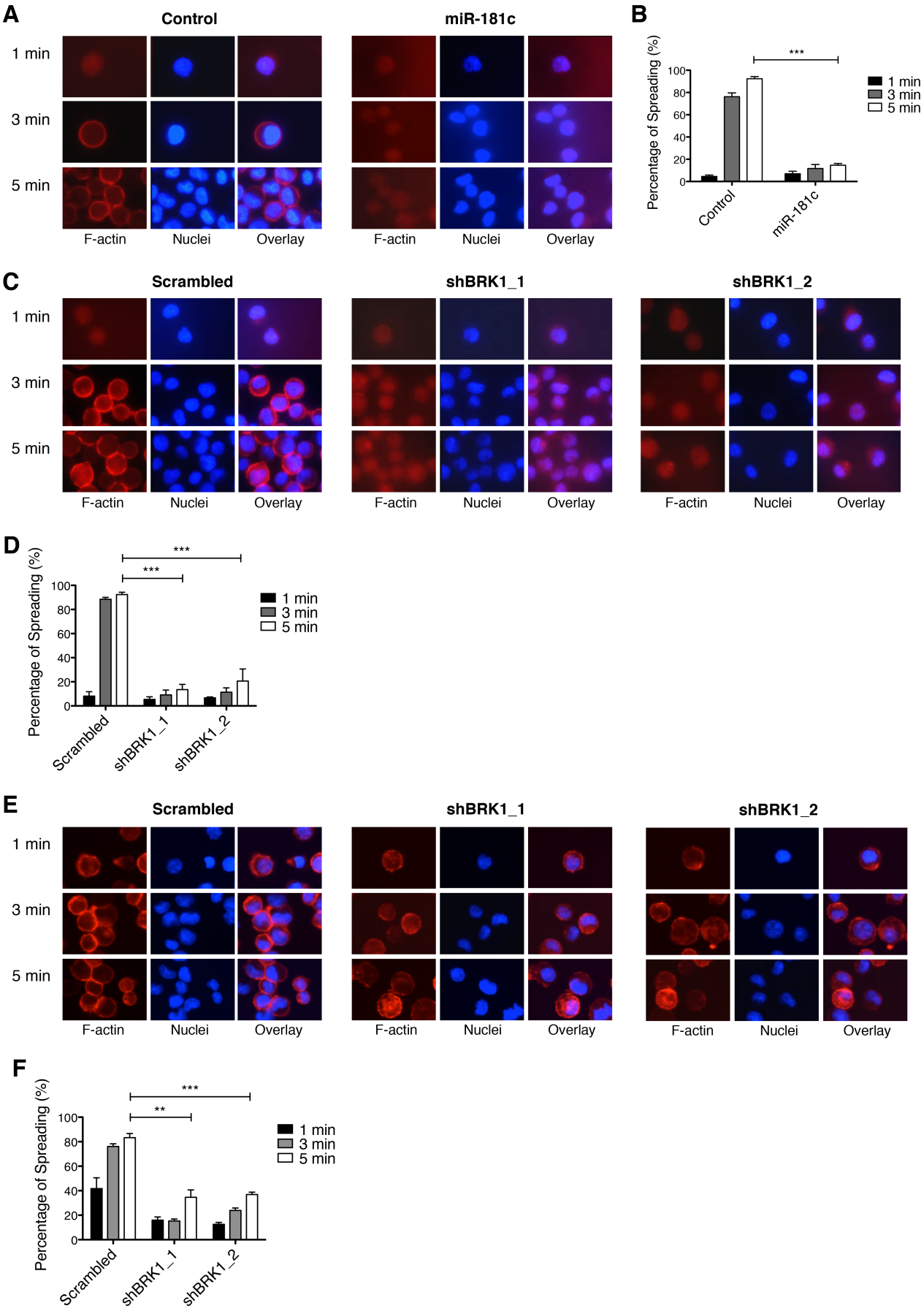
A
Control
miR-181c
1 min
3 min
5 min
F-actin
Nuclei
Overlay
B
Percentage of Spreading (%)
***
1 min
3 min
5 min
Control
miR-181c
C
Scrambled
shBRK1_1
shBRK1_2
D
Scrambled
shBRK1_1
shBRK1_2
E
Scrambled
shBRK1_1
shBRK1_2
F
**

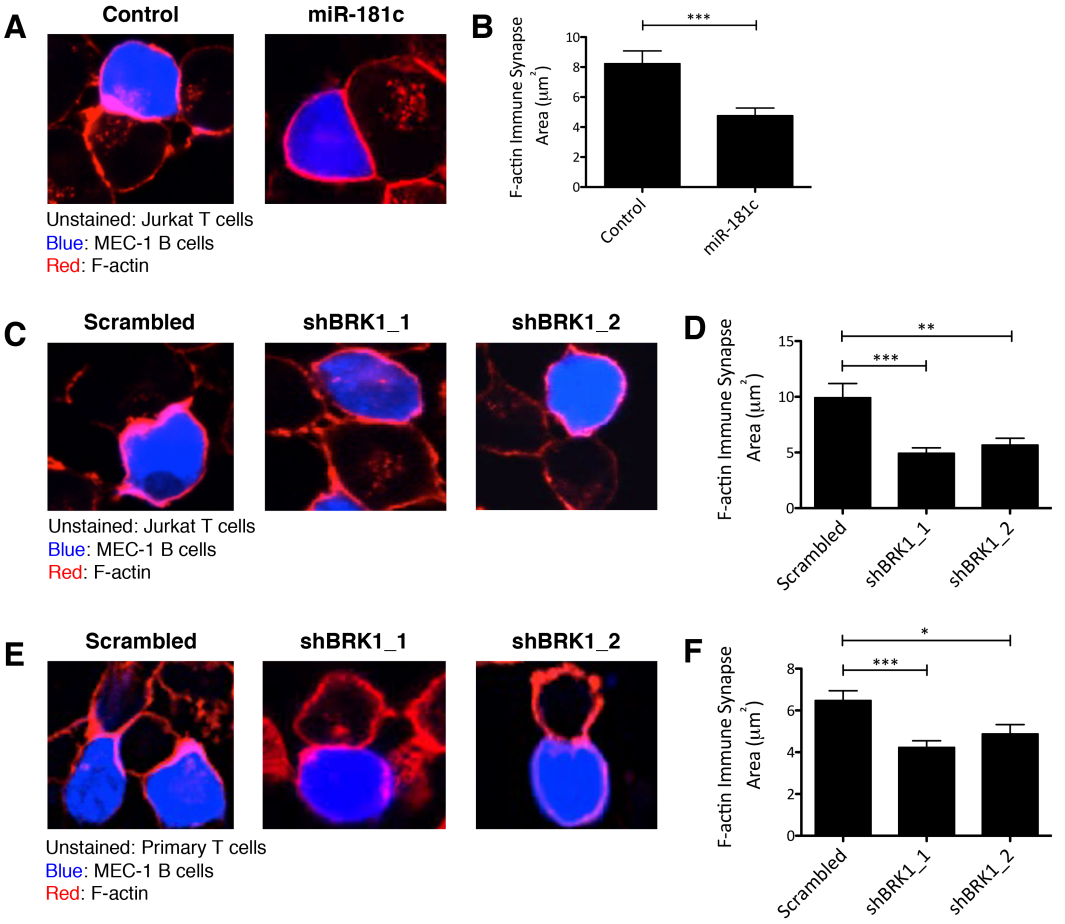
A
Control
miR-181c
Unstained: Jurkat T cells
Blue: MEC-1 B cells
Red: F-actin
B
F-actin Immune Synapse Area (μm²)
***
Control
miR-181c
C
Scrambled
shBRK1_1
shBRK1_2
Unstained: Jurkat T cells
Blue: MEC-1 B cells
Red: F-actin
D
F-actin Immune Synapse Area (μm²)
**
***
Scrambled
shBRK1_1
shBRK1_2
E
Scrambled
shBRK1_1
shBRK1_2
Unstained: Primary T cells
Blue: MEC-1 B cells
Red: F-actin
F
F-actin Immune Synapse Area (μm²)
*
***
Scrambled
shBRK1_1
shBRK1_2